The Effect of Bulk Composition on the Sulfur Content of Cores

by

Hannah L. Bercovici

A Thesis Presented in Partial Fulfillment
of the Requirements for the Degree
Master of Science

Approved April 2020 by the
Graduate Supervisory Committee:

Linda Elkins-Tanton, Chair
Laurence Garvie
Meenakshi Wadhwa

ARIZONA STATE UNIVERSITY

May 2020

ABSTRACT

This study explores how bulk composition and oxygen fugacity (fO_2) affect the partitioning of sulfur between the molten mantle and core of an early planetesimal. The model can be used to determine the range of potential sulfur concentrations in the asteroid (16) Psyche, which is the target of the National Aeronautics and Space Administration/Arizona State University Psyche Mission. This mission will be our visit to an M-type asteroid, thought to be dominantly metallic.

The model looks at how oxygen fugacity (fO_2), bulk composition, temperature, and pressure affect sulfur partitioning in planetesimals using experimentally derived equations from previous studies. In this model, the bulk chemistry and oxygen fugacity of the parent body is controlled by changing the starting material, using ordinary chondrites (H, L, LL) and carbonaceous chondrites (CM, CI, CO, CK, CV). The temperature of the planetesimal is changed from 1523 K to 1873 K, the silicate mobilization and total melting temperatures, respectively; and pressure from 0.1 to 20 GPa, the core mantle boundary pressures of Vesta and Mars, respectively.

The final sulfur content of a differentiated planetesimal core is strongly dependent on the bulk composition of the original parent body. In all modeled cores, the sulfur content is above 5 weight percent sulfur; this is the point at which the least amount of other light elements is needed to form an immiscible sulfide liquid in a molten core. Early planetesimal cores likely formed an immiscible sulfide liquid, a eutectic sulfide liquid, or potentially were composed of mostly troilite, FeS.

DEDICATION

For my human family: Julie, David, Sarah, and Giulia.

For my dog family: Eppy, Bella, Juno, Remy, Canyon, and Max.

For my advisors: Lindy, Karen, and my other mentors who helped me figure out what I want to do and who I want to be.

For my friends: Glenna, Mitch, and all the other amazing people who have supported me along the way.

And *for myself.*

"All you have is what you are, and what you give."

~ Ursula Le Guin, *The Dispossessed*

ACKNOWLEDGMENTS

This research was supported by the NASA Psyche Mission awarded to the Psyche Team in 2017 and the ASU Graduate College Fellowship 2018-2019. Special thanks to my collaborators and advisors, Linda Elkins-Tanton, Joseph O'Rourke, Laura Schaefer, Tim McCoy, Laurence Garvie, and the many others who helped me with coding, finding data, and thinking through various modeling issues. Thank you to Hilairy Hartnett for providing comments and filling in for Mini on my committee.

TABLE OF CONTENTS

Page

LIST OF TABLES

Table Page

LIST OF FIGURES

LIST OF EQUATIONS

Equation Page

CHAPTER 1

INTRODUCTION

The asteroid (16) Psyche, the target of the NASA Psyche mission, is hypothesized to be partly metallic. Psyche could be (1) unprocessed primordial material; (2) an impacted body that is a mixture of core and mantle components; or (3) a partially stripped planetesimal (Elkins-Tanton et al., 2020). The asteroid is likely dominated by a variety of materials: from a mixture of core and mantle components to a new type of chondritic material not represented in our meteorite collections, though potentially similar to CB chondrites (Elkins-Tanton et al., 2020). This study attempts to determine the sulfur content of core material derived from a variety of chondrite precursors that are thought to be among the first minimally processed solids to form in the Solar System (Elkins-Tanton et al., 2011 and references therein).

The Psyche mission is expected to provide insights into the processes that form metal-rich asteroids, a type of body unexplored until now (Scheinberg et al., 2016; Elkins-Tanton et al., 2017). Planetesimals are thought to be the building blocks of planets, and so understanding Psyche's formation is vital to understanding the components that build larger planets like Earth (Bottke et al., 2006; Elkins-Tanton et al., 2020). Planetesimals formed in varied environments, reflected by different compositions, oxygen fugacities, and temperatures, which affect their geochemical signatures, and thus can affect the geochemistry of larger planets such as Earth (e.g., Elkins-Tanton et al., 2017; Kruijer et al., 2017; Desch et al., 2018). This study models the effect of bulk composition, oxidation state (i.e., fO_2), temperature, and pressure on core formation in

planetesimals. In particular, we want to understand how sulfur, a significant component in planetary cores, partitions between the core and mantle during differentiation (Kilburn and Wood, 1997; Suer et al., 2017). Our predictions will be useful in interpreting geochemical data from the Psyche mission and understanding the geochemical processes that may have occurred in early planetesimal cores.

Magmatic iron meteorites are thought to be pieces of cores from differentiated parent bodies. Age models using radiogenic isotopes suggest these meteorites formed between 0.5 to 1 Ma years after CAI formation (Kleine et al., 2005; Scherstén et al., 2006), and potentially even earlier than the CAI's (Goldstein et al., 2009). Sulfur typically exhibits siderophile properties and as such is thought to be a significant light element in planetary cores, including the Earth's (Kracher and Wasson, 1982; Murthy and Hall, 1970; Suer et al., 2017). Models of trace element trends in iron meteorites indicate that between 2 and 18 weight percent (wt.%) of sulfur must have been present during core crystallization (Chabot, 2004; Goldstein et al., 2009; Walker et al., 2008). Trace elements, such as Ir and Ga, in iron meteorites show compositional trends that imply they behaved like chalcophiles during core crystallization. These trends suggest that an immiscible sulfide liquid was present during core crystallization (Ulff-Møller, 1998; Chabot, 2004; Goldstein et al., 2009).

Despite the expectation of sulfur's presence in early planetesimal cores, the measured bulk sulfur content of existing magmatic iron meteorites is significantly lower than their modeled sulfur contents (Ulff-Møller, 1998; Chabot, 2005; Goldstein et al., 2009), and only found in the form of troilite (FeS) or other sulfides (e.g., Buchwald, 1975; Moore et al., 1968; Ulff-Møller, 1998; Wasson, 1999; Chabot, 2004; Wasson et al., 2007; Walker

et al., 2008; Goldstein et al., 2009). Some studies have explained the absence of sulfur by suggesting it escaped the core through an immiscible sulfide liquid prior to the collisions that created our iron meteorite collection (Ulff-Møller, 1998; Chabot, 2004; Goldstein et al., 2009). While sulfur generally prefers to remain in metallic rather than silicate liquids, sulfur is incompatible in Fe-Ni metal. As such, sulfur could have formed an immiscible sulfide liquid as its concentration increased in the melt during core crystallization (Goldstein et al., 2009).

Sulfur forms an immiscible liquid at concentrations greater than 47 wt.% sulfur in a pure Fe-S melt (Waldner and Pelton, 2005). In a metallic melt that contains >1 wt.% other light elements (such as C, Si, or P), a sulfide immiscible liquid will form when the sulfur concentration reaches ~5 wt.%. However, immiscible liquids can form at even lower sulfur contents depending on other light element concentrations (Jones and Drake, 1983; Poirier, 1994; Corgne et al., 2008). The critical point for immiscible sulfide liquid formation in a Fe-Ni melt with <1 wt.% other light elements is >15 wt.% S (Ulff-Møller, 1998). However, because pure sulfide is structurally weak, any sulfide-dominant meteorite is likely to have decomposed before reaching our meteorite collection (Kracher and Wasson, 1982). Alternatively, we may not yet have sulfide-dominant meteorites due to a lack of sampling from all parts of the asteroid belt (McSween, 1999), though non-magmatic iron meteorites such as group IAB do have high amounts of sulfur (>10 wt.%), more than magmatic ones (Wasson and Kallemeyn, 2002).

The partitioning behavior of sulfur has not yet been modeled at the thermodynamic conditions relevant to planetesimals. Previous studies have modeled how sulfur affects trace element partitioning in planetesimals (e.g., Chabot, 2004; Mungall et al., 2005;

Goldstein et al., 2009; Wade, Wood and Tuff, 2012; Steenstra et al., 2016; Wang and Becker, 2017), and how sulfur partitions in Mars- and Earth-sized planets (e.g., Kilburn and Wood, 1997; Stewart and Schmidt, 2007; Mahan et al., 2017; Suer et al., 2017). However, no studies have specifically focused on sulfur in planetesimals with radius <300 km in radii or internal pressures <1 GPa.

After determining the effect of temperature and pressure on the sulfur partition coefficient, we model the effects of bulk composition and oxidation state on core sulfur content and core size. We use chondritic compositions from Jarosewich (1990, 2006) to determine how the original parent body's bulk composition and oxidation state influence the sulfur partition coefficient. The dataset reported in Jarosewich (2006) has the advantage of being a single source dataset obtained with consistent methods, described in Jarosewich (1990). We recognize other datasets contain more analyses of the chondrites used in this study. However, in consideration of using data that was collected through consistent methods, we decide to only use the Jarosewich (2006) dataset.

We use the compositions of several chondrites as examples of the starting materials from which differentiated planetesimals may have formed. Though some early planetesimals could have been partially differentiated and thus contain a metal core (e.g., Elkins-Tanton et al., 2011), as suggested for the IAB and winonaite parent body (Kracher, 1985), partial differentiation is not the focus of this study. We are not suggesting that iron meteorites came directly from the cores of specific chondritic parent body. Instead, we use the chondritic compositions as the material from which the hypothetical planetesimals formed. We show that while parameters such as temperature, pressure, bulk composition, and oxidation state influence the silicate-metal partition

coefficient of sulfur, the bulk composition is the main controller of the size and sulfur content of the core.

MODELS AND METHODS

Modeling the effect of temperature, pressure and bulk composition on Ds.

A planetary body should form a core above the melting and mobilization temperature of silicates in a chondritic body (i.e., 1523 K, McCoy et al., 1997). At the liquidus temperature of silicates (i.e., 1873 K in a CV-chondrite bulk composition, McCoy et al., 1997), a metallic liquid will be able to form a core in all planetesimal types, regardless of oxidation state. Therefore, in this study we model the effect of temperature from 1523 K to 1873 K on the partition coefficient of sulfur.

We consider core formation through percolation at the Fe-FeS eutectic (i.e., 1223 K, Terasaki et al., 2008), as percolation likely occurred in small planetesimals prior to silicate melting, as suggested for lodranites, acapulcoites, and winonaites (Kracher, 1985; McCoy et al. 1997, Terasaki et al., 2008; Goldstein et al., 2009). When a core forms at 1223 K, we assume that all the sulfur goes into the core. In the absence of molten silicate, the partition coefficient does not apply because the slow diffusion timescales for solids will limit the extent of thermodynamic equilibration during core formation. We then compare the sulfur content of a core that forms at the Fe-FeS eutectic to the sulfur content of a core that forms after silicates begin to melt.

We also model how sulfur's partition coefficient (D_S) varies from 0.1 GPa to 20 GPa, which are the predicted core-mantle boundary pressure for Vesta (Righter and Drake, 1996), and 20 GPa the core-mantle boundary pressure for Mars (Fei et al., 1995). By

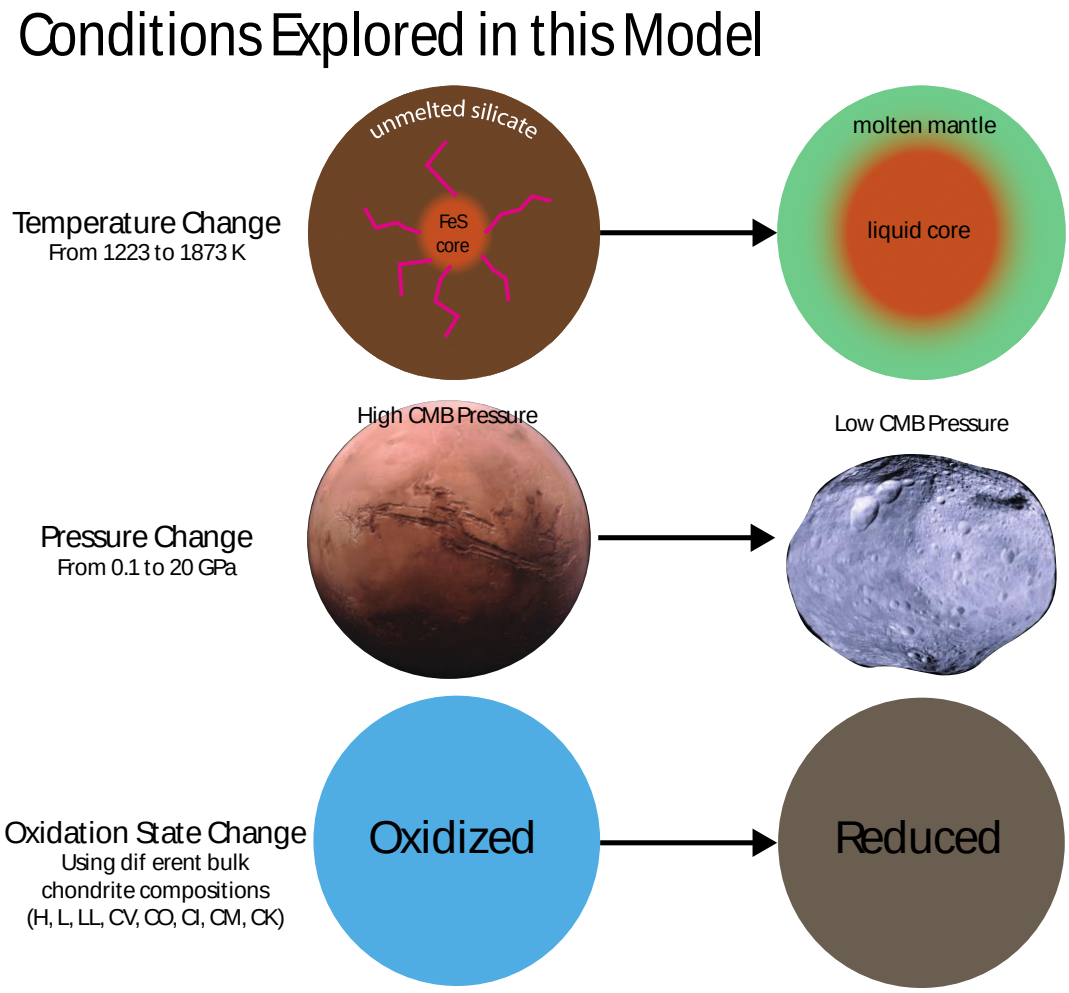

Figure 1. The three parameters (temperature, pressure, and oxygen fugacity) used to model the effect the sulfur content on core formation. Images of Mars and Vesta are from NASA (Mars - solarsystem.nasa.gov; Vesta - nasa.gov/mission_pages/dawn).

looking at this range of core-mantle boundary pressures, we are able to show the behavior of sulfur in a range of small planetesimals.

Sulfur partitions between the core and molten mantle according to:

$$Ds = \frac{X_S^{core}}{X_S^{mantle}} \qquad \text{[eq. 1]},$$

where X_S^{core} is the mole fraction of sulfur in the liquid core and X_S^{mantle} is the mole fraction of sulfur in the molten mantle (Li and Agee, 2001; Rose-Weston et al., 2009; Boujibar et al., 2014; Suer et al., 2017).

Various studies have determined the effects of temperature and pressure on sulfur's partition coefficients (Li and Agee, 2001; Rose-Weston et al., 2009; Boujibar et al., (2014); Suer et al., (2017). Most studies used pressures above 1 GPa and temperatures above 2000 K. While Suer et al. (2017) use experiments at pressures between 46 and 91 GPa to determine sulfur's partition coefficient, which is significantly higher than for planetesimals and planetary embryos, we chose to use the parameterization from Suer et al. (2017) for several reasons. Unlike earlier studies such as Rose-Weston et al. (2009), Suer et al. (2017) extended their parameterization to low pressure values and considered oxidation state, which is an important parameter in our study. Suer et al. (2017) do not explicitly consider the effects of light elements other than sulfur in the core, and they suggest that the inclusion of other light elements in Boujibar et al. (2014) made sulfur's partitioning behavior too complicated to reproduce accurately in a model. In addition, Suer et al. (2017) derive their equation by combining their experiments with other studies, excluding Boujibar et al. (2014), and extrapolate *Ds* for pressures from 1 to 100 GPa. As no low-pressure experiments are available that derive the partition coefficient of sulfur, we use the equation for *Ds* that Suer et al. (2017):

$$log\ Ds = -3.3 + \frac{3000}{T} + 14\left(\frac{P}{T}\right) + log\ X_{FeO}^{mantle} - log\ C_s \qquad \text{[eq. 2]},$$

where T is temperature in Kelvin, P is pressure in GPa, X_{FeO}^{mantle} is the mole fraction of FeO in the molten mantle, and C_S is the sulfide capacity of the molten mantle (Haughton et al., 1974; Suer et al., 2017).

The sulfide capacity, *Cs*, is defined as the saturation point for sulfides in the molten silicates; that is the maximum sulfur content the molten silicate fraction can accommodate before sulfides begin to precipitate. The sulfide capacity is primarily affected by the ferrous iron content of the silicates, which in turn is affected by the bulk composition and oxidation state of the parent body (Haughton et al., 1974). The equation for sulfide capacity is (e.g., Haughton et al., 1974):

$$C_S = X_S^{mantle} * (\frac{fO_2}{fS_2})^{\frac{1}{2}} \qquad \text{[eq. 3]},$$

where X_S^{mantle} is the mole fraction of sulfur in the molten mantle, fO_2 is the oxygen fugacity, and fS_2 is the sulfur fugacity.

As the mole fraction of sulfur in the molten mantle (X_S^{mantle}) and the core (X_S^{core}) are unknowns in this study, we cannot calculate a theoretical mantle sulfide capacity using Equation 3. Instead, we use an experimentally derived equation for *Cs* that depends on the oxide content of the molten mantle (Haughton et al., 1974):

$$logC_S = -5.705 + 3.15X_{FeO}^{mantle} + 2.65X_{CaO}^{mantle} + 0.12X_{MgO}^{mantle} + 0.77X_{TiO_2}^{mantle} + 0.75(X_{Na_2O}^{mantle} + X_{K_2O}^{mantle}) \qquad \text{[eq. 4]},$$

where X_M^{mantle} is the mole fraction of oxide in the silicate mantle. We account for oxygen fugacity using the ferrous iron content of the molten mantle that correlates with oxygen fugacity and most strongly affects Cs (Haughton et al., 1974).

Oxidation State.

We use eight different chondrites as the initial bulk compositions for our modeled differentiated planetesimals (Table 1). We do not use enstatite chondrites, the most reduced chondrite group (Wadhwa, 2008 and references therein), because Jarosewich

(2006) did not report an iron oxide content for enstatite chondrites, a value needed for our calculation of *Ds*.

The oxygen fugacity of each chondritic bulk composition is calculated relative to the iron-wüstite (ΔIW) buffer using equation 5 from (Darken and Gurry, 1946):

$$\Delta IW = 2log\left(\frac{X_{FeO}^{mantle}}{X_{Fe}^{core}}\right) \qquad \text{[eq. 5]},$$

where X_{Fe}^{core}, the mole fraction of iron in the core, is assumed to equal the original amount of metallic iron (Fe^0) in the bulk parent body (Table 1). Our calculated oxidation states reproduce the oxidation sequence reported in the literature (Righter et al., 2007; Righter et al., 2016; Schrader et al., 2017; Wadhwa, 2008).

Table 1. Average bulk compositions of the chondrites with one sigma population error (standard deviation divided by the square root of the number of analyses). Meteorite data from Jarosewich (2006). Oxygen fugacity was calculated from Darken and Gurry (1946).

Chondrite Type	FeO wt.%	Fe (metal) wt.%	Ni (metal) wt.%	FeS wt.%	fO_2 (ΔIW)
H	13 ± *0.64*	13 ± *0.68*	1.7 ± *0.02*	5.2 ± *0.08*	-1.4± *0.05*
L	15 ± *0.24*	6.1 ± *0.22*	1.2 ± *0.01*	5.6 ± *0.11*	-1.2 ± *0.02*
LL	17 ± *0.47*	2.6 ± *0.68*	0.93 ± *0.08*	5.3 ± *0.32*	-0.93 ± *0.05*
CV	24 ± *3.1*	0.89 ± *0.77*	0.40 ± *0.20*	3.2 ± *0.79*	-0.55 ± *0.20*
CO	24 ± *1.9*	2.3 ± *0.94*	1.2 ± *0.31*	5.2 ± *1.2*	-0.54 ± *0.14*
CI	17 ± *n/a*	0 ± *n/a*	0 ± *n/a*	9.1 ± *n/a*	-0.36 ± *n/a*
CM	23 ± *0.95*	0.06 ± *0.02*	0.26 ± *0.17*	7.1 ± *0.59*	-0.27 ± *0.04*
CK	28 ± *0.39*	0.27 ± *0.03*	1.1 ± *0.14*	2.8 ± *0.33*	-0.22 ± *0.01*

Calculating core sulfur content and size.

In our study, we assume that only iron, nickel, and sulfur partition into the core. However, other light elements, such as phosphorus, also likely partition into the core.

While we understand there is some partitioning into the core for most elements listed in oxide form below, most are generally minor. For simplicity, we assume all oxides remain in the mantle. To determine the sulfur content of the mantle and core after differentiation, we begin by defining which oxides are in the mantle versus the core:

Mantle: $(FeO+SiO_2+Al_2O_3+MgO+NaO+CaO+K_2O+P_2O_5+TiO_2+MnO)_y(S)_z$, and

Core: $(Fe)_a(Ni)_b(S)_c$; therefore,

Total sulfur: z + c = B.

Then, we define the partition coefficient (Equation 1) according to:

$$D_S = \frac{c/(a+b+c)}{z/(y+z)},$$

$$D_S = \frac{c}{z} * (\frac{y+z}{a+b+c}), \text{ and}$$

$$D_S = \frac{c}{B-c} * (\frac{y+B-c}{a+b+c}).$$

Simplifying variables:

$$\alpha = y + B, \text{ and}$$

$$\beta = a + b,$$

we find that:

$$D_S = \frac{c}{B-c} * (\frac{\alpha-c}{\beta+c}),$$

$$D_S = \frac{-c^2+\alpha c}{-c^2+(B-\beta)c+B\beta},$$

is a quadratic function of the sulfur content of the core:

$$(1 - D_s)c^2 + [(B - \beta)D_S - \alpha]c + B\beta D_s = 0.$$

Further simplifying variables:

$$\gamma = 1 - D_S,$$

$$\theta = (B - \beta)D_S - \alpha, \text{ and}$$

$$\Phi = B\beta D_S.$$

We can solve for sulfur content of the core in moles:

$$c = \frac{-\theta - \sqrt{\theta^2 - 4\gamma\Phi}}{2\gamma} \qquad \text{[eq. 6]},$$

as the negative form of the quadratic formula is the only one to give us a real value.

Therefore, the mole fraction of sulfur in the core is:

$$X_S^{core} = \frac{c}{a+b+c} \qquad \text{[eq. 7]}.$$

Lastly, after calculating the mass of sulfur in the core, we determine the radius of the core and the radius of the planetesimal.

To determine the radius of the core and planetesimal, we first calculate the density of the mantle following Kaus et al. (2005). We assume the mantle composition is a Hawaiian plagioclase lherzolite because it is the type of peridotite that forms at the lowest pressure and a good representation of a small planetesimal mantle well. In addition, we assume the mantle of a small planetesimal has not been depleted in any elements and the Hawaiian lherzolite tends to be less depleted than other types of peridotite. We calculate the mantle density following (e.g., Kaus et al., 2005):

$$\rho_{mantle} = 3388(1 - 3.4 \times 10^{-5}T + 1.34 \times 10^{-11}P) \qquad \text{[eq. 8]},$$

where ρ_{mantle} is the density of the mantle, T is temperature (298 K to mimic a cooled planetary body), and P is the pressure at the core-mantle boundary (0.1 GPa for a Vesta-sized planetesimal; Righter and Drake, 1996).

For the core density, we assumed that the cores of the modeled planetesimals are composed of taenite (7.5 wt.% Ni, 94 wt.% Fe), with a density of ~7.81 g/cm3 (Furnish et al., 1994), and troilite, with a density of 4.61 g/cm3 (Firdu and Taskinen, 2010).

We then calculated the densities of the different cores as:

$$\rho_{core} = F_{FeS}^{core} * \rho_{FeS} + (1 - F_{FeS}^{core}) * \rho_{\gamma} \qquad \text{[eq. 9]},$$

where ρ_{core} is the density of the core, F_{FeS}^{core} is the mass fraction of troilite in the core, ρ_{FeS} is the density of troilite, and ρ_{γ} is the density of taenite. We calculated the volume of the core and the parent body using the modeled densities from Eqs. (8) and (9). The radius fraction of the core relative to the parent body was calculated from the volume. We determined the respective radii of the Fe-Ni-rich and sulfur-rich portions of the core through the same process (see Fig. 7).

RESULTS

Temperature and Pressure.

Temperature and pressure have opposite effects on the partition coefficient of sulfur, but both have negligible effects on the sulfur content of the core. The sulfur partition coefficient has an inverse relationship with temperature (Fig. 2). Sulfur thus becomes more lithophile at higher temperatures. In contrast, the sulfur partition coefficient increases with pressure (Fig. 3).

When we change both pressure and temperature, we find that sulfur has a very high partition coefficient, >100, indicating that the majority of the sulfur in the parent body will partition into the core rather than the mantle (Fig. 2 and 3). Therefore, neither pressure nor temperature strongly affect the sulfur content of planetesimal cores. The body with the highest partition coefficient is derived from L-chondrites, which is considered more reduced than all but the H-chondrites. The L-chondrite derived body has

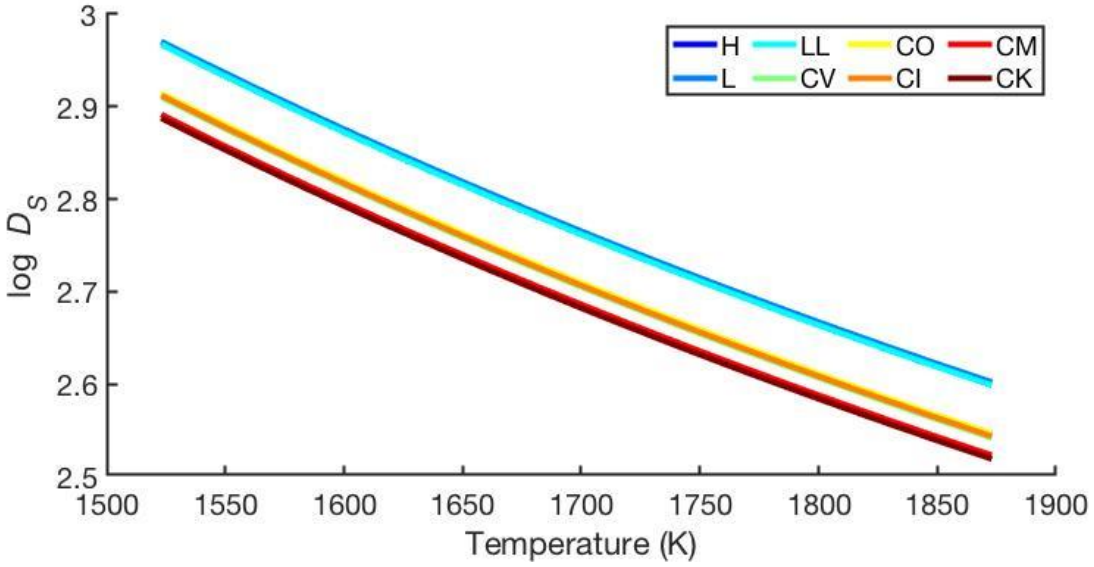

Figure 2. Partition coefficient of sulfur, *Ds*, as a function to temperature (K) at 0.1 GPa. The partition coefficient of sulfur decreases with increasing temperature, though the sulfur content of the core does not change significantly because for all bulk compositions and temperatures the partition coefficient is above 100.

an average oxygen fugacity of ~ΔIW-1.2, at 0.1 GPa, and the L-derived body's *Ds* value falls from 934 at 1532 K to 400 at 1873 K (Fig. 2).

Of the compositions studied, the CK chondrites have the lowest partition coefficient, with an oxygen fugacity about one log unit higher than that of the L chondrite at ~ΔIW-0.2. The CK-derived mean partition coefficient changes from 772 to 330 between 1532 and 1873 K at P = 0.1 GPa (Fig. 2). However, these differences in *Ds* result in little change in the sulfur content of the core because all the calculated partition coefficients calculated are large and positive. In fact, we find that all modeled cores from 1223 K (the Fe-FeS eutectic) to 1873 K (the silicate melting temperature) have only a 1 to 4% difference in sulfur content. Pressure also has a minimal effect on the sulfur content of

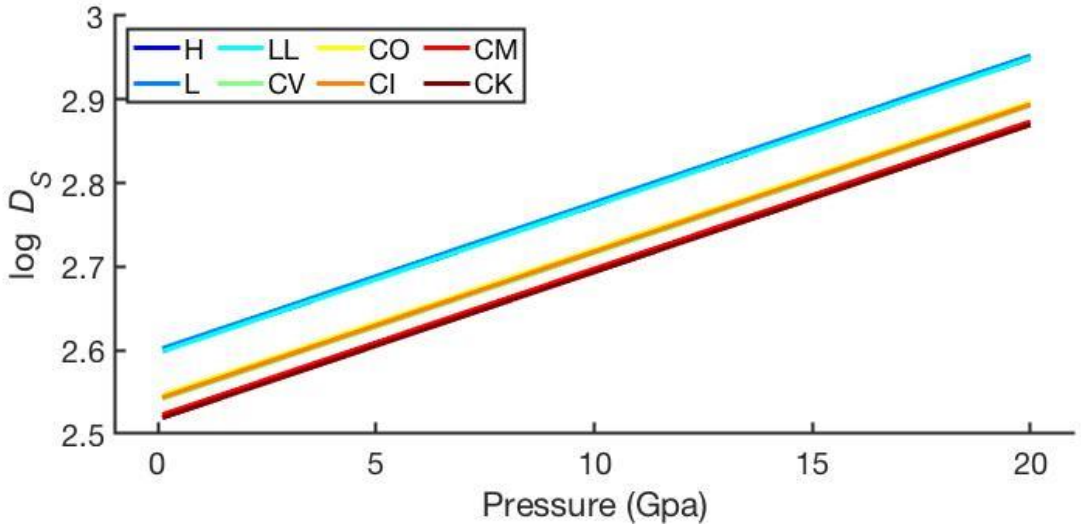

Figure 3. Partition coefficient of sulfur, *Ds*, as a function of pressure (GPa) at 1873 K. The partition coefficient of sulfur increases as pressure increases from 0.1 GPa, the lowest core mantle boundary pressure for our modeled planetesimals (Righter and Drake, 1996), to 20 GPa, the likely core-mantle boundary (CMB) pressure for Mars (Fei et al., 1995).

the core; we find less than a 2% difference in core sulfur content between 0.1 and 20 GPa at T = 1873 K for all modeled cores.

Oxygen fugacity.

Bulk composition determines fO_2 (Fig. 4) and is the main controller on the sulfur content of the core and on core size (Table 2; Fig. 5). Metallic iron and iron oxide show opposite relationships with oxygen fugacity (Fig. 4A and B), as expected considering how we calculated the oxidation state (Eq. 5). However, the FeS content of the bulk parent body has no relationship to oxidation state (Fig. 4C). As chondrite FeS content is seemingly independent of fO_2, we then determined whether oxidation state affects sulfur's partition coefficient.

Table 2. Normalized class average modeled core compositions with one sigma population error. Meteorite data from Jarosewich (2006). Oxygen fugacity calculated using Darken and Gurry (1946).

Chondrite Type	Fe wt.%	Ni wt.%	S wt.%	Radius % of core to parent body
H	82.2 ± *0.933*	8.37 ± *0.475*	9.42 ± *0.477*	49.4 ± *0.642*
L	74.9 ± *0.539*	9.41 ± *0.332*	15.7 ± *0.333*	42.6 ± *0.354*
LL	67.9 ± *1.35*	10.6 ± *0.703*	21.5 ± *1.10*	37.9 ± *1.25*
CV	65.9 ± *3.67*	8.83 ± *2.06*	25.3 ± *3.12*	30.8 ± *4.31*
CO	64.6 ± *3.38*	14.0 ± *3.66*	21.4 ± *2.89*	38.3 ± *3.61*
CI	63.9 ± *n/a*	0 ± *n/a*	36.1 ± *n/a*	46.5 ± *n/a*
CM	62.2 ± *1.33*	3.51 ± *2.10*	34.4 ± *0.781*	40.1 ± *0.914*
CK	49.9 ± *0.658*	26.6 ± *1.27*	23.5 ± *0.819*	29.4 ± *1.15*

Our calculations show that while T, P, and fO_2 all affect the D_S (Fig. 2, 3, 5A), the bulk composition of the starting chondritic materials has the primary effect on the core size and sulfur content (Fig. 5B and C). As oxidation increases, the mean partition coefficient decreases. This relationship is consistent across equations used to determine the partition coefficient of sulfur, including those of Boujibar et al. (2014), who considered light elements in their calculations.

All modeled bodies form cores with greater than 6 wt.% sulfur (Fig. 5B). The core with the least sulfur is H-chondrite derived, with 6.5 wt.% sulfur. The core with the greatest amount of sulfur is from the CI-chondrite derived body (Table 2) and incorporates up to 36 wt.% sulfur (Fig. 5B; Table 2). The iron and sulfur content of the cores have an inverse relationship until ~65 wt.% Fe, when cores either contain about 65 wt.% Fe and contain more sulfur (up to 35 wt.%) or contain about 25 wt.% S and decrease in Fe (Fig. 6). This tells us that the iron and sulfur contents of the core are the main controllers of core characteristics, such as size, as the largest cores either contain

the most sulfur (CI-derived) or iron (H-derived) (Fig. 5C, 6). Bulk composition of the parent body is the main controller of the sulfur content and size of the core.

The CV-derived bodies form the smallest cores at a minimum value of 6% radius fraction (Fig. 5C). The CI-derived body forms a core at 41% of the parent body radius, larger than the more reduced LL and L chondrites, which have mean radius percentages of 35% and 40%, respectively (Fig. 5C; Table 2). The smallest cores, like in a few CV-chondrite compositions, derive from compositions and therefore cores with little metallic iron and iron sulfide (Table 1, Fig. 6, 7). Some cores, derived from CK- and CV-chondrite-derived bodies, contain comparable amounts of iron and sulfur, and so their modeled core sizes are controlled by both elements.

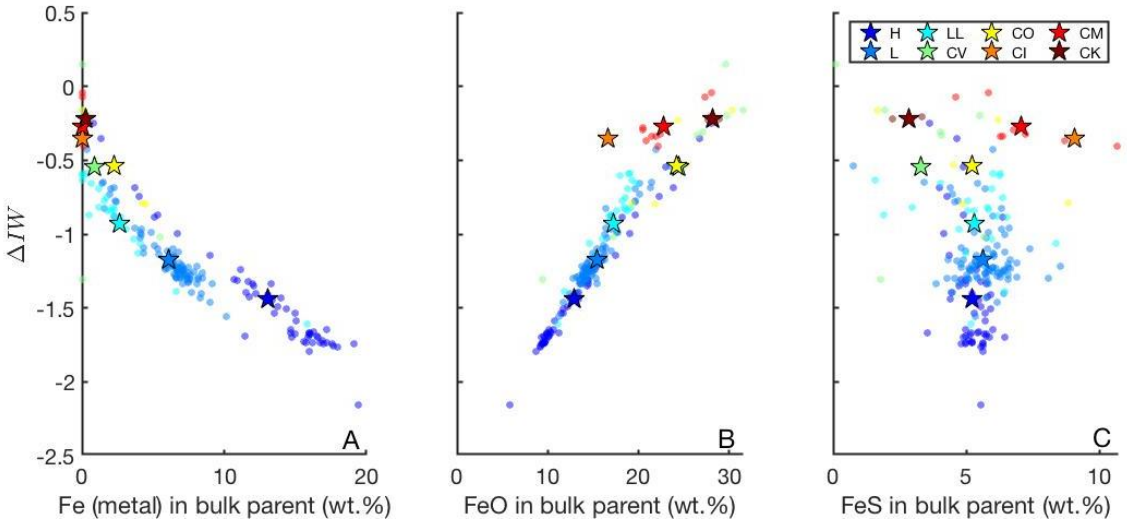

Figure 4. Iron sulfide does not show a relationship with oxygen fugacity, while iron, in both oxidized and metallic forms, is strongly related to the oxidation state of the parent body. This figure shows the parent body oxidation state as a function of Fe (a), FeO (b), and FeS (c). Individual chondrite compositions are shown as points and their class average are an outlined star of the same color (compositions from Jarosewich, 2006).

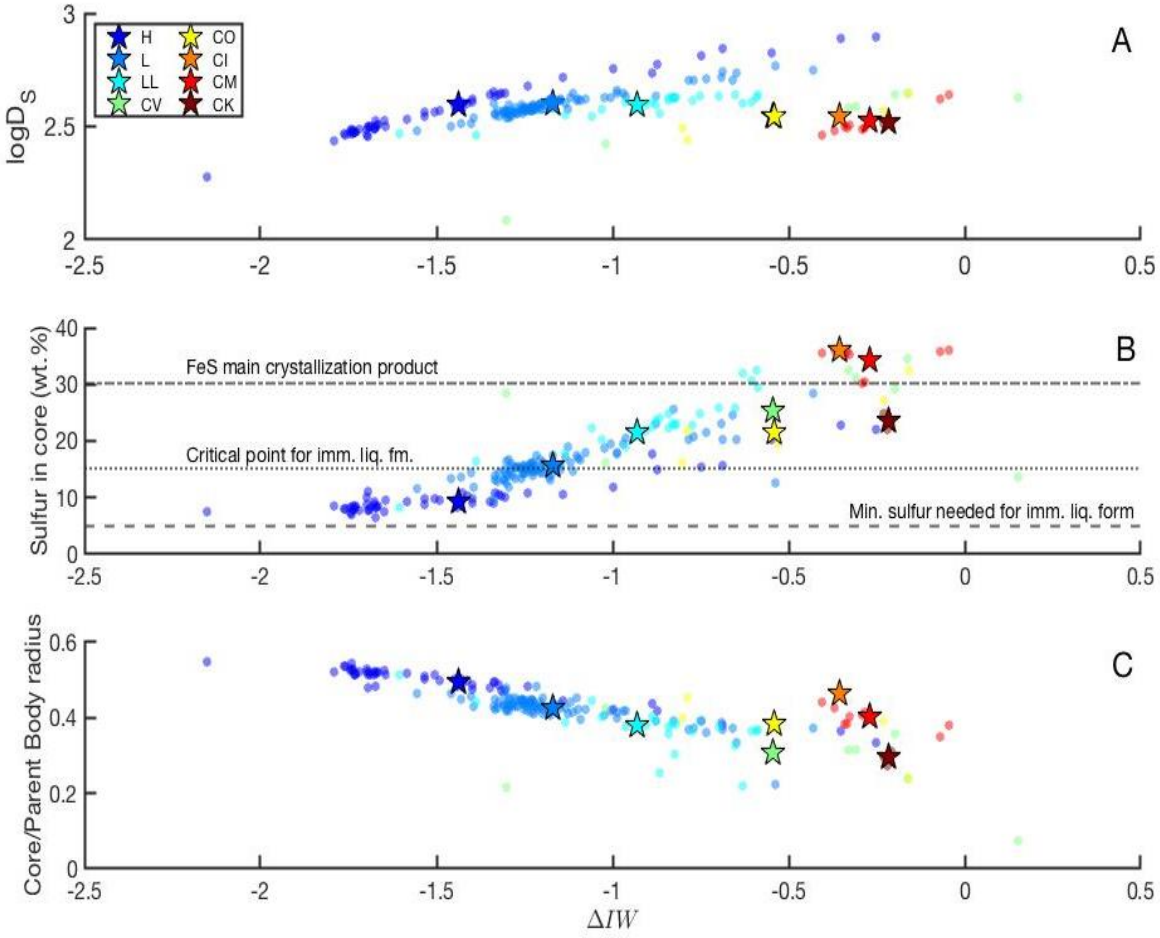

Figure 5. The bulk composition has the greatest effect on the sulfur content and size of the core. These plots show the effects of A) log of the sulfur partition coefficient; B) core sulfur concentration with lines for the crystallization of FeS (>30 wt.% S, Waldner and Pelton, 2005), the critical point for sulfide immiscible liquid formation (>15 wt.% S and <1 wt.% other light elements, Ulff-Møller, 1998), and low-sulfur sulfide immiscible liquid formation (5 wt.% S, >1 wt.% other light elements); and C) core size relative to the oxidation state. Individual chondrite compositions are shown as points and their class averages are an outlined star of the same color (data from Jarosewich, 2006). The temperature in this run is 1873 K and the pressure is 0.1 GPa.

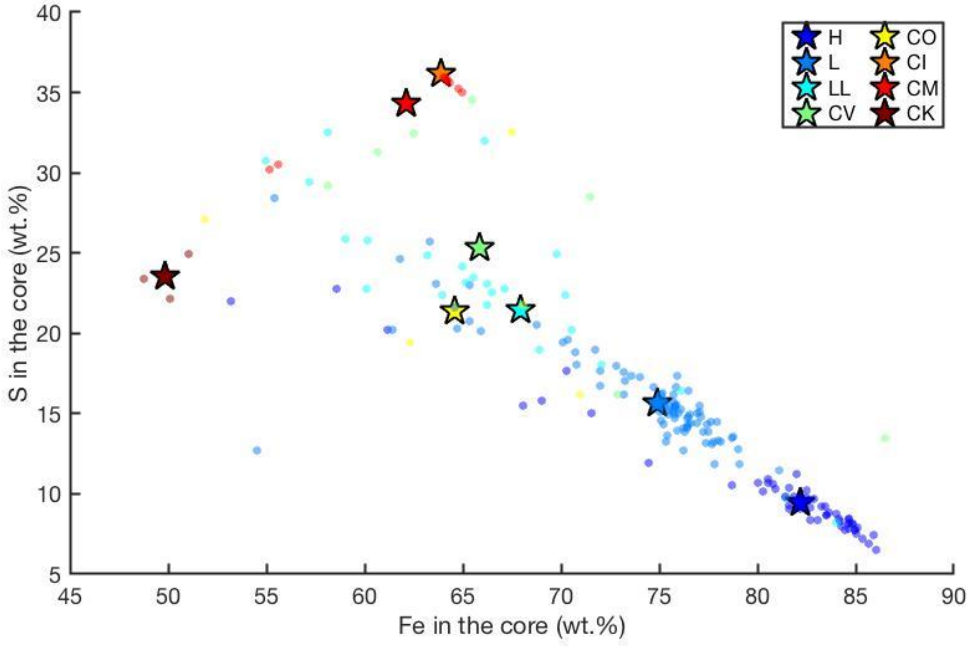

Figure 6. The iron content of the modeled cores decreases with increasing sulfur content, except for CK-derived cores that are more affected by the nickel content of the core. Individual chondrite compositions are shown as points and their class averages are an outlined star of the same color (Jarosewich 2006).

DISCUSSION

The results of our calculations show that bulk parent-body composition has the largest influence on the sulfur content and size of a core (Fig. 4-6). As a parent-body becomes more oxidized, its bulk composition contains more silicates, less free metal, and therefore less core-forming material. However, the sulfur content of the core does not appear to be affected by oxidation state (Fig. 5), but rather is strongly correlated with bulk composition (Fig. 6, 7).

Our modeling is consistent with planetesimal cores forming an immiscible sulfide liquid, assuming that light elements, such as C, P, and Si are present in the core. If >1

wt.% of light elements besides sulfur are present, a sulfide immiscible liquid can form before core crystallization in our modeled cores because they all contain >5 wt.% S (Jones and Drake, 1983; Corgne et al., 2008; Fig. 5B). If <1 wt.% other light elements are present, then the Fe-Ni liquid would have to reach >15 wt.% S (Ulff-Møller, 1998), which is true for all of our cores except those derived from H-chondrites. During crystallization, the Fe-Ni melt will likely contain >15 wt.% S, especially once it reaches its monotectic temperature, and will form a sulfide liquid that will then escape the core.

The delayed formation of a separate sulfide liquid supports models by Chabot (2004) and others that suggest sulfur was present in cores during crystallization and explains the lack of sulfur in the current collection of magmatic iron meteorites. In addition, the formation of an immiscible sulfide liquid in other cores prior to crystallization can also explain the lack of sulfur present during fractionation in certain iron meteorite groups, like IVB irons (Walker et al., 2008). The immiscible sulfide liquid in either case will be buoyant relative to the Fe-Ni metal, and form a sulfide outer core; such is postulated for Mercury and for IIIAB iron meteorites (Ulff-Møller, 1998; Harder and Schubert, 2001; Hauck et al., 2006).

In order to understand which of our cores could have produced meteoritic compositions, we plot our modeled cores at 1873 K, the iron meteorite compositions (Buchwald, 1975; Walker et al., 2008; Wasson and Richardson, 2001; Wasson, 1999; Wasson and Huber, 2006; Wasson et al., 2007) and experimental core compositions (Chabot, 2004) on a Fe/Ni/S ternary diagram (Fig. 8 and 9). To approximate the removal of a sulfur-rich immiscible liquid, we removed sulfur from our modeled core compositions as iron sulfide (65 wt.% Fe, 29 wt.% S, and 5.1 wt.% Ni; Jones and Drake,

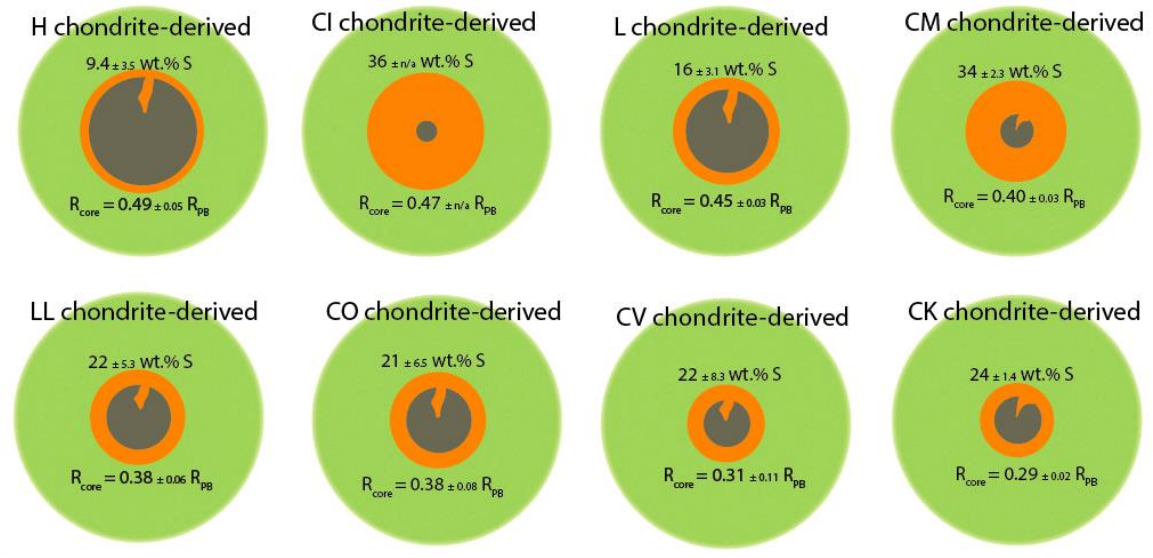

Figure 7. The modeled cores of each class average contain above 5 wt.% sulfur, resulting in the formation of an immiscible sulfide liquid in most cores; or in the case of CI- and CM-derived bodies, the formation of a troilite dominant core. Here the class average modeled cores are in size order and labeled with their chondritic precursor. Note that they are not in fO_2 order. The bodies are colored according to the fraction of silicate (green), sulfur (orange), and iron + nickel (grey).

1983). The composition of the liquid in the metallic core becomes Fe- and Ni-rich with the removal of the sulfide immiscible liquid (Fig. 8).

Both H- and L-derived core liquids becomes more Fe-rich with the removal of a sulfide immiscible liquid, and the others become more nickel rich (Fig. 8). The CI-, CM-, and, CK-derived core liquids are not shown because their core compositions are more sulfur-rich than stoichiometric troilite, and therefore produce only liquid FeS. Extra sulfur could react with iron and form pyrite once cooled, though pyrite is unknown in iron meteorites (Raghavan, 2004).

The modeled core compositions and sulfur-depleted modeled core compositions overlap with those of natural samples and natural samples with a sulfide immiscible

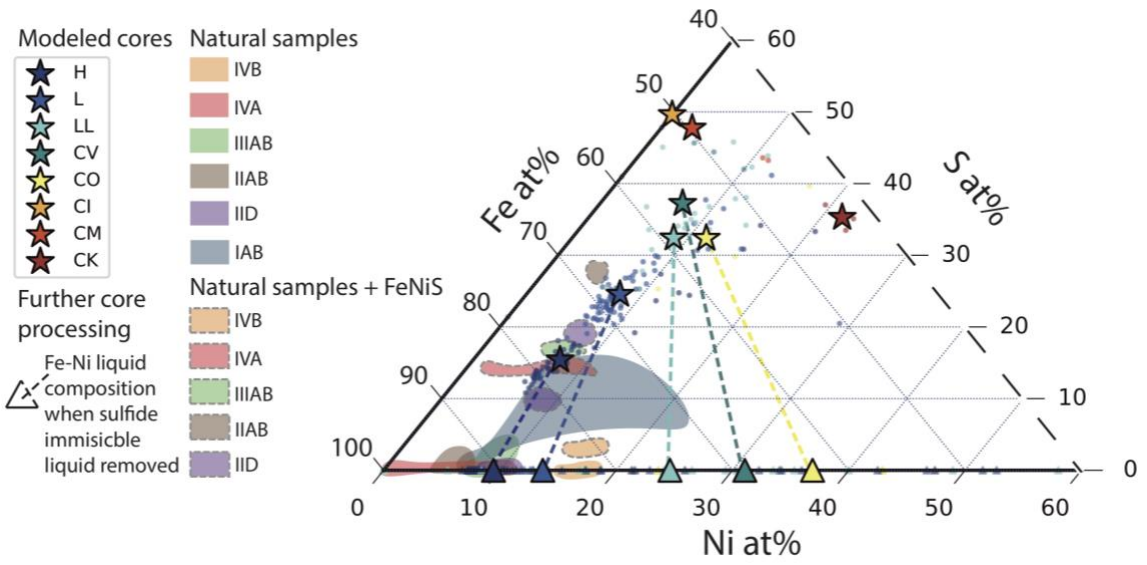

Figure 8. The loss of a sulfur-rich immiscible liquid from relatively more reduced modeled cores in this study produces core compositions consistent with values found in previous studies. Shaded regions represent natural samples found in our meteorite collection (Buchwald, 1975; Wasson, 1999; Wasson and Richardson, 2001; Wasson and Kallemeyn, 2002; Wasson and Huber, 2006; Wasson et al., 2007; Walker et al., 2008). Individual modeled cores are represented by colored circles, and the class average of each chondrite is represented by stars of corresponding colors. Outlined and shaded regions are iron meteorite compositions with sulfur added back into them according to modeled predictions (Ulff-Møller, 1998; Chabot, 2004; Goldstein et al., 2009). The composition of the sulfide is from Jones and Drake (1983). Triangles represent the Fe-Ni liquid composition when an immiscible sulfide liquid is removed from the core. The immiscible liquid composition is taken from Jones and Drake (1983) and subtracted from the modeled core composition. Dashed lines tie together the modeled core compositions and the S-free Fe-Ni liquid compositions.

liquid added back to them (Fig. 8). Modeled compositions of H-, L-, and LL- derived cores that undergo no sulfur loss at 1873 K overlap with the predicted compositions from IID, IIIAB, IIAB, and IVA iron meteorites. H-chondrite derived modeled cores also overlap with IAB main group compositions; these very sulfur-rich non-magmatic iron meteorites that are thought to represent a core that formed through partial melting (Kracher, 1985; Schulz et al., 2012).

The H-, L-, LL-, and CV-derived cores that undergo sulfur depletion above 5 wt.% sulfur at 1873 K overlap with all included iron meteorites (Fig. 8). More oxidized core types, i.e., LL, CV, and CO contain high levels of Ni, which can overlap with some iron meteorites, though these are not included in this figure. For example, ungrouped iron meteorites like Tishomingo and Dermbach contain over 30 wt.% Ni (Buchwald, 1975), and IAB-ungrouped Oktibbeha County contains ~60 wt.% Ni (Wasson and Kallemeyn, 2002). By removing sulfur via a sulfide immiscible liquid, the compositions of sulfide-depleted modeled cores from more reduced bodies are similar to iron meteorite compositions. We also find that experimental planetesimal core compositions from Chabot et al. (2003) overlap with our modeled cores derived from H-, L-, LL-, and CV-chondrites (Fig. 9).

Cores of planetesimals likely contained sufficient concentrations of light elements to have produced a sulfur-rich immiscible liquid that would have buoyantly separated from the Fe-Ni liquid prior to fractionation, or at the monotectic temperature. We also explore a scenario where no light elements are present in the liquid. In this case the core would fractionate with sulfur in its main liquid until the Fe-FeS eutectic at ~50 at.% S (Raghavan, 2004). We modeled fractional solidification of the bulk core material from 1173 K to 1873 K, removing the phases indicated by Raghavan (2004). For example, in a chondrite derived core, only taenite crystallizes, while in a CI-chondrite derived core, only iron sulfide crystallizes.

Overall, the liquid paths in pure Fe-Ni-S do not overlap with the compositions of meteorites, except those of the H- chondrite derived material (Fig. 10). The liquid path of the average H-derived core overlaps with IIAB, IIIAB, and IID iron meteorites. This

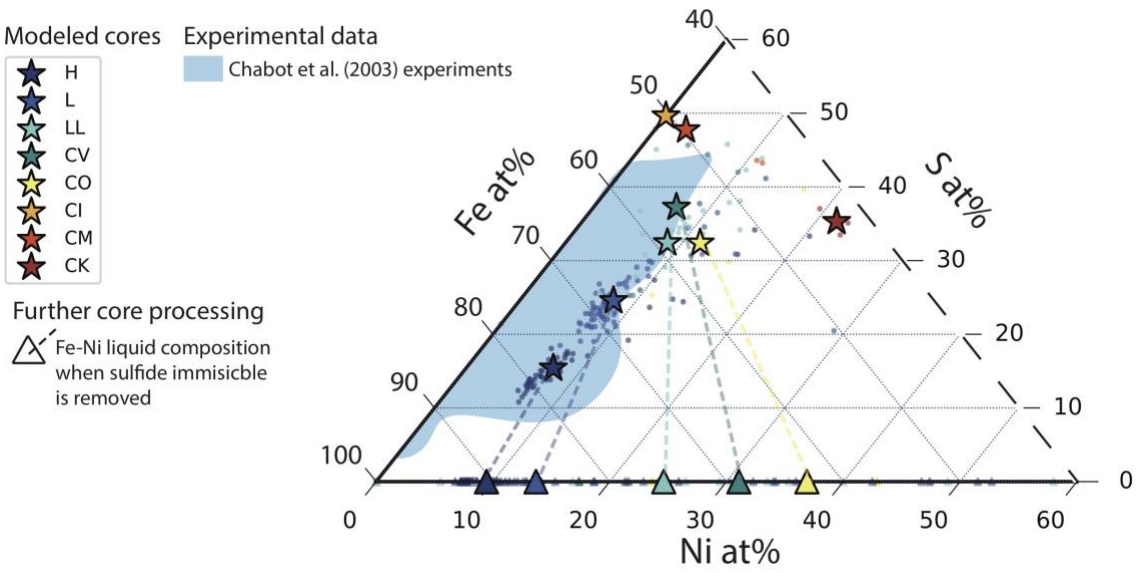

Figure 9. Modeled cores from more reduced planetesimals (H, L, LL, and CV) overlap with experiments conducted by Chabot et al. (2003). The blue shaded field represents the most likely Fe-Ni-S contents of planetesimal cores prior to sulfide loss (Chabot et al., 2003). Individual modeled cores are represented by colored circles, and the class average of each chondrite-type is represented by stars of corresponding colors. Like in Figure 8, triangles represent the Fe-Ni liquid composition when a sulfide immiscible liquid is removed.

overlap suggests these iron meteorites did not reach immiscibility until fractionation began, but then lost sulfur as the liquid reached a composition closer to the critical point of immiscibility, described further in Ulff-Møller (1998). Most of the iron meteorites explored in our study likely experienced some form of sulfur loss prior to fractionation, in agreement with Chabot et al. (2003), Chabot (2004), and Goldstein et al. (2009).

Our model also explains the lack of sulfur in meteorites that are thought to be more oxidized and depleted in light elements, such as the IVB group of iron meteorites (Kruijer et al., 2017; Walker et al., 2008). Walker et al. (2008) and Chabot (2004)

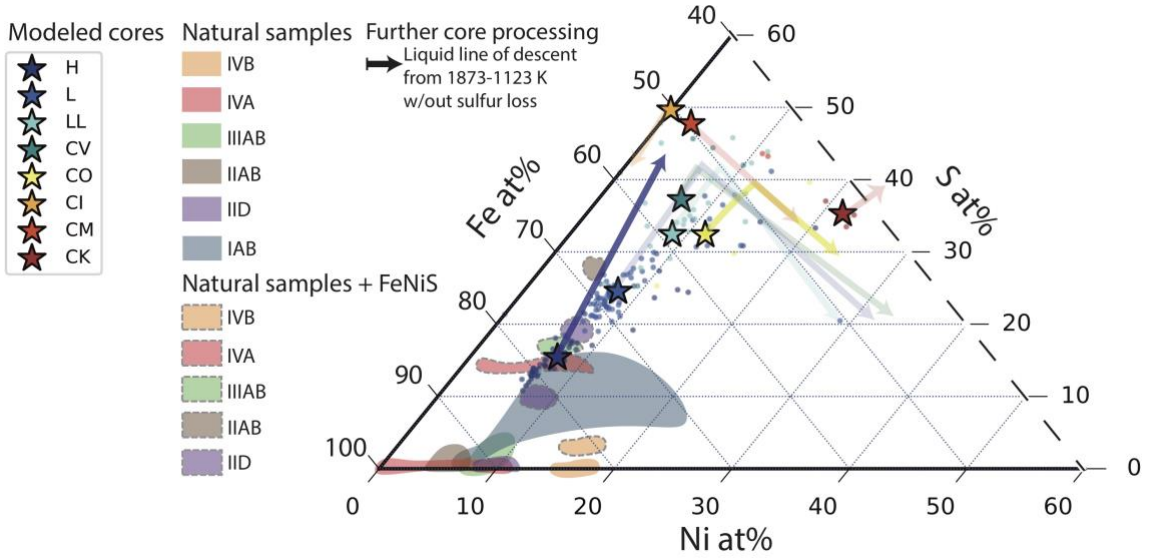

Figure 10. When sulfur remains in the core during crystallization, only H-derived cores overlap with iron meteorite compositions that have Fe-Ni sulfide added back in. Individual modeled cores are represented by colored circles, and the class average of each chondrite-type is represented by stars of corresponding colors. Lines with arrows show the direction of the liquid lines of descent for each class average core liquid. The modeled core composition represents the liquid at 1873 K, which is crystallized to 1123 K according to Fe-Ni-S phase diagrams in Raghavan (2004). Shaded regions are described in Figure 9.

showed that the trace-element trends are consistent with <2 wt.% S present during core crystallization. Several studies interpret this result to imply the absence of sulfur during core formation (Ulff-Møller, 1998; Chabot and Drake, 1999; Chabot, 2004; Walker et al., 2008; Goldstein et al., 2009). However, our model suggests oxidized bodies will potentially have higher concentrations of sulfur in their cores. We suggest that a sulfide-immiscible liquid could have separated from the liquid Fe-Ni metal prior to crystallization in the parent bodies that eventually formed the IVB irons (Fig. 8). For example, if a small planetesimal formed with a 1 bar CMB pressure, <1 wt.% P and ~15 wt.% sulfur would be needed to form an immiscible sulfide liquid (Ulff-Møller, 1998).

The IVB irons could have lost light elements, including sulfur, to an immiscible sulfide liquid before crystallization.

Other irons, such as in the IVA group, could derive from a bulk composition similar to H-chondrites that lost all of its sulfur prior to fractionation (Fig. 8). Thus, most of our iron meteorite collection could come from more reduced chondrite-derived planetesimals that lost sulfur.

Troilite cores?

The relatively oxidized parent bodies, such as CI- and CM-type, contain sulfur and iron metal that stoichiometrically match troilite (Fig. 4-6). However, the question arises as to whether troilite is dense enough to sink through an FeO-rich magma ocean to form a core. The silicate magma ocean of a carbonaceous parent body would be dense due to a high iron oxide content (Fu and Elkins-Tanton, 2014). Carbonaceous chondritic bodies can form melts with densities up to 2.88 g/cm$_3$ at 1473 K (see Fig. 4 in Fu and Elkins-Tanton, 2014). Molten troilite reaches a density of 3.8 g/cm$_3$ at 1473 K (Firdu and Taskinen, 2010), and therefore would sink to the center of the body. At this time, no observational evidence supports this conclusion for troilite cores, other than the IAB iron meteorites that are considered to be non-magmatic (Kracher, 1985).

There is no overlap between magmatic iron meteorites and our more oxidized modeled cores (Fig. 8). The absence of such material may imply that cores from carbonaceous chondrite-type planetesimals have not yet been sampled, due to the fact our meteorite collection represents an incomplete sampling of the asteroid belt (McSween, 1999). One group of non-magmatic iron meteorites, IAB, is theorized to come from the

core of a partially melted planetesimal that theoretically contained between 5-25 wt.% sulfide (Kracher, 1985; Schulz et al., 2012). The IAB group could also represent the core of an oxidized planetesimal that experienced either partial or total melting, as a core is likely to form in an oxidized body in both cases (Terasaki et al., 2008). However, troilite cores are thought to be structurally weak and would only require one significant collision to be destroyed (Kracher, 1985). In addition, if we did receive a piece of a troilite core, any trace of these potential meteorites could also be lost to weathering (Kracher and Wasson, 1982). Sulfide meteorites (and cores) may very well exist, but we either have not sampled them yet or they were destroyed long ago and decomposed before we found them.

Implications for Psyche.

The composition of Psyche is unknown, and many theories exist for what the asteroid could be: from a disrupted rubble pile to a metal-rich chondrite (Elkins-Tanton et al., 2020). It is also possible that it is a new type of body not yet present in our meteorite collections. Some potential scenarios include:

1. If an immiscible sulfide liquid was present in Psyche *after* it was stripped of its mantle, this liquid could have risen through the Fe-Ni metal and flooded the surface. This sulfide deposit could still be detectable if it was not stripped away or was protected by the topography of the asteroid.
2. If an immiscible sulfide liquid formed as a layer between the mantle and the core (i.e., Fig. 7), then it could be detectable on Psyche's surface in the scenario that Psyche is a disrupted and rearranged planetesimal.

3. If Psyche's parent body contained about equimolar metallic iron and sulfur, then the asteroid could be made mostly of Fe-Ni sulfide. This could apply to certain meteorites we see in our collection, like the IAB iron meteorites (Kracher, 1985; Schulz et al., 2012) that are assumed to be non-magmatic but could be from a mostly differentiated oxidized parent body. This could especially be the case as oxidized bodies can form cores at lower temperatures than reduced bodies (Kracher, 1985; Terasaki et al., 2008). However, we also think this would be unlikely, as sulfide-dominant cores are thought to be structurally weak and thus easily destroyed (Kracher, 1985).

The density of cooled troilite is 4.62 g/cm$_3$ (Firdu and Taskinen, 2010), which is within the range of densities for Psyche. Most recently, the Psyche team has consolidated the available data and determined the density of the asteroid to be 3.78 ± 0.34 g/cm$_3$; this value best represents the current state of our knowledge (Elkins-Tanton et al., 2020). One explanation for the low density is that Psyche could be a porous troilite core (5-20 vol% porosity, Elkins-Tanton et al., 2020). If Psyche is in fact a core, it could represent the samples we already find in our meteorite collection, or it could be a sample of a core we never would have expected to discover.

CONCLUSIONS

We show that the molten cores expected to form from chondritic precursors will contain more than 5 wt.% sulfur, which is the lower bound for the formation of an immiscible sulfide liquid. If a planetesimal core forms either at the Fe-FeS eutectic or after silicate mobility, an immiscible sulfide liquid will likely form. The sulfide liquid can then escape

the core, regardless of the initial conditions of planetesimal formation and differentiation. Further, in the case that a core does not reach immiscibility until a critical point as suggested by Ulff-Møller (1998), a sulfide immiscible liquid would likely still form once crystallization commences. Once the liquid contains above 15 wt.% S, with as little as 0.6 wt.% P present, an immiscible sulfide liquid will form. These two points of immiscibility explain why some iron meteorites crystallized with a significant amount of sulfur in their systems, and that sulfur was subsequently lost (Chabot, 2004; Goldstein et al., 2009), and why some, like IVB iron meteorites, appeared to have cooled with very little sulfur present (Walker et al., 2008).

Alternatively, if sulfur remained in the core until after crystallization, perhaps it escaped through overpressurization or ferrovolcanism, which are predicted to have potentially occurred on Psyche (Abrahams and Nimmo, 2019; Johnson et al., 2019). These predictions mostly considered an iron-rich melt, and should be further studied and tested with sulfur in the melt (Abrahams and Nimmo, 2019; Johnson et al., 2019). Some of our modeled cores retained their sulfur as they cooled and overlapped with a few iron meteorite compositions (Fig. 10). This overlap suggests the sulfur content of the core was affected by multiple processes occurring in early planetesimal cores, supporting findings by Chabot et al. (2003). In addition, some carbonaceous chondrite-derived planetesimals formed cores at the iron-sulfide eutectic (>30 wt.% S), suggesting that sulfide would be the main solid that formed during crystallization. As a result, cores dominated by troilite may be able to form in oxidized planetesimals.

Four main conclusions can be drawn from this research.

1. All modeled partition coefficients are large and positive (>100), indicating that most sulfur partitions into the core in our explored cases.
2. Bulk compositions with low levels of bulk metallic iron (<1 wt.% Fe) form differentiated bodies with small, sulfur-rich cores. Compositions with high levels of sulfides (>9 wt.% FeS) can form large, sulfur-rich cores. Compositions with high bulk iron (>9 wt.% Fe) form large, Fe-rich cores.
3. During differentiation, planetesimal cores can form a sulfide-rich immiscible liquid prior to fractionation or soon after crystallization begins.
4. The compositions of iron meteorite groups explored in this study can be explained by processes including the formation of an immiscible sulfide liquid in core from a more reduced planetary body. In addition, IAB iron meteorites could be the remnants of a core from an oxidized planetesimal core, whether through partial or total melting.

WORKS CITED

Abrahams, J. N. H., and Nimmo, F. (2019). Ferrovolcanism: Iron Volcanism on Metallic Asteroids. *Geophysical Research Letters*, *46*, 2019GL082542.

Agee, C. B., Li, J., Shannon, M. C., and Circone, S. (1995). Pressure-temperature phase diagram for the Allende meteorite. *Journal of Geophysical Research*, *100*, 17725–17740.

Bottke, W. F., Nesvorný, D., Grimm, R. E., Morbidelli, A., and O'Brien, D. P. (2006). Iron meteorites as remnants of planetesimals formed in the terrestrial planet region. *Nature*, *439*(7078), 821–824.

Boujibar, A., Andrault, D., Bouhifd, M. A., Bolfan-Casanova, N., Devidal, J. L., and Trcera, N. (2014). Metal-silicate partitioning of sulphur, new experimental and thermodynamic constraints on planetary accretion. *Earth and Planetary Science Letters*, *391*(April), 42–54.

Buchwald, V. F. (1975). *Handbook of Iron Meteorites* (Vol. 1).

Chabot, N. L., Campbell, A. J., Jones, J. H., Humayun, H., and Agee, C. B. (2003). An experimental test of the Henry's law in solid metal-liquid metal systems with implications for iron meteorites. *Meteoritics and Planetary Science*, *38*(2), 181–196.

Chabot, Nancy L. (2004). Sulfur contents of the parental metallic cores of magmatic iron meteorites. *Geochimica et Cosmochimica Acta*, *68*(17), 3607–3618.

Corgne, A., Wood, B. J., and Fei, Y. (2008). C- and S-rich molten alloy immiscibility and core formation of planetesimals. *Geochimica et Cosmochimica Acta*, *72*(9), 2409–2416.

Darken, L. S., and Gurry, R. W. (1946). The System Iron-Oxygen. II. Equilibrium and Thermodynamics of Liquid Oxide and Other Phases. *Journal of the American Chemical Society*, *68*(5), 798–816.

Desch, S. J., Kalyaan, A., and Alexander, C. M. O. (2018). The Effect of Jupiter's Formation on the Distribution of Refractory Elements and Inclusions in Meteorites. *The Astrophysical Journal Supplement Series*, *238*(1), 11.

Elkins-Tanton, L.T., Asphaug, E., Bell III, J. F., Bercovici, D., Bills, B. G., Binzel, R. P., … Zuber, M. T. (2017). Asteroid (16) Psyche: Visiting a Metal World. *LPSC 2017*.

Elkins-Tanton, Linda T., Weiss, B. P., and Zuber, M. T. (2011). Chondrites as samples of differentiated planetesimals. *Earth and Planetary Science Letters*, *305*(1–2), 1–10.

Elkins-Tanton, L. T., Asphaug, E., Bell, J. F., Bercovici, H., Bills, B., Binzel, R., … Zuber, M. T. (2020). Observations, meteorites, and models: A pre-flight assessment

of the composition and formation of (16) Psyche. *Journal of Geophysical Research: Planets*, (16), 2019JE006296.

Fei, Y., Prewitt, C. T., Mao, H. K., and Bertka, C. M. (1995). Structure and density of FeS at high pressure and high temperature and the internal structure of Mars. *Science*, *268*(5219), 1892–1894.

Firdu, F. T., and Taskinen, P. (2010). *Densities of Molten and Solid Alloys of*. Retrieved from https://pdfs.semanticscholar.org

Fu, R. R., and Elkins-Tanton, L. T. (2014). The fate of magmas in planetesimals and the retention of primitive chondritic crusts. *Earth and Planetary Science Letters*, *390*, 128–137.

Furnish, M. D., Iii, G. T. G., Remo, J. L. J. L., Gray III, G. T., and Remo, J. L. J. L. (1994). Dynamical Behavior of Octahedrite from the Henbury Meteorite. *AIP Conference Proceedings*, *309*.

Goldstein, J. I., Scott, E. R. D., and Chabot, N. L. (2009). Iron meteorites: Crystallization, thermal history, parent bodies, and origin. *Chemie Der Erde - Geochemistry*, *69*(4), 293–325.

Harder, H., and Schubert, G. (2001). Sulfur in Mercury's Core? *Icarus*, *151*, 118–122.

Hauck, S. A., Aurnou, J. M., and Dombard, A. J. (2006). Sulfur's impact on core evolution and magnetic field generation on Ganymede. *Journal of Geophysical Research*, *111*(E9), E09008.

Haughton, D. R., Roeder, P. L., and Skinner, B. J. (1974). *Solubility of Sulfur in Mafic Magmas*. Retrieved from https://pubs.geoscienceworld.org/segweb/economicgeology/article-pdf/69/4/451/3484790/451.pdf

Jarosewich, E. (1990). Chemical analyses of meteorites: A compilation of story and iron meteorite analyses. *Meteoritics*, *25*, 323–337.

Jarosewich, Eugene. (2006). Chemical analyses of meteorites at the Smithsonian Institution: An update. *Meteoritics and Planetary Science*, *41*(9), 1381–1382.

Johnson, B. C., Sori, M. M., and Evans, A. J. (2019). Ferrovolcanism on metal worlds and the origin of pallasites. *Nature Astronomy*, 1–4.

Jones, J. H., and Drake, M. J. (1983). Experimental investigations of trace element fractionation in iron meteorites. III: Elemental partitioning in the system Fe-Ni-S-P. *Geochimica et Cosmochimica Acta*, *47*, 1199–1209.

Kaus, B. J. P., Connolly, J. A. D., Podladchikov, Y. Y., and Schmalholz, S. M. (2005). Effect of mineral phase transitions on sedimentary basin subsidence and uplift. *Earth and Planetary Science Letters*, *233*(1–2), 213–228.

Kilburn, M. R., and Wood, B. J. (1997). Metal–silicate partitioning and the incompatibility of S and Si during core formation. *Earth and Planetary Science Letters*, *152*, 139–148.

Kleine, T., Mezger, K., Palme, H., Scherer, E., and Munker, C. (2005). Early core formation in asteroids and late accretion of chondrite parent bodies: evidence from 182Hf–182W in CAIs, metal-rich chondrites, and iron meteorites. *Geochemica et Cosmochimica Acta*, *69*, 5805–5818.

Kracher, A. (1985). The evolution of partially differentiated planetesimals: Evidence from iron meteorite groups IAB and IIICD. *Journal of Geophysical Research*, *90*(S02), 689–698.

Kracher, A., and Wasson, J. T. (1982). The role of S in the evolution of the parental cores of the iron meteorites. *Geochimica et Cosmochimica Acta*, *46*(12), 2419–2426.

Kruijer, T. S., Burkhardt, C., Budde, G., and Kleine, T. (2017). Age of Jupiter inferred from the distinct genetics and formation times of meteorites. *Proceedings of the National Academy of Sciences*, 201704461.

Li, J., and Agee, C. B. (2001). Element partitioning constraints on the light element composition of the Earth' core. *Geophysical Research Letters*, *28*(1), 81–84.

Mahan, B., Siebert, J., Pringle, E. A., and Moynier, F. (2017). Elemental partitioning and isotopic fractionation of Zn between metal and silicate and geochemical estimation of the S content of the Earth's core. *Geochemica et Cosmochimica Acta*, *196*, 252–270.

McCoy, T. J., Keil, K., Muenow, D. W., and Wilson, L. (1997). Partial melting and melt migration in the acapulcoite–lodranite parent body. *Geochemica et Cosmochimica Acta1*, *61*, 639–650.

McSween, H. Y. (1999). *Meteorites and Parent Planets*.

Moore, C. B., Lewis, C. F., and Nava, D. (1968). Superior Analyses of Iron Meteorites. In *Meteorite Research* (pp. 738–748).

Mungall, J. E., Andrews, D. R. A., Cabri, L. J., Sylvester, P. J., and Tubrett, M. (2005). Partitioning of Cu, Ni, Au, and platinum-group elements between monosulfide solid solution and sulfide melt under controlled oxygen and sulfur fugacities. *Geochimica et Cosmochimica Acta*, *69*(17), 4349–4360.

Murthy, V. R., and Hall, H. T. (1970). The chemical composition of the Earth's core: Possibility of sulphur in the core. *Physics of the Earth and Planetary Interiors*, *2*(4), 276–282.

Poirier, J.-P. (1994). Light elements in the Earth's outer core: A critical review. *Physics of the Earth and Planetary Interiors*, *85*(3–4), 319–337.

Raghavan, V. (2004). Fe-Ni-S (iron-nickel-sulfur). *Journal of Phase Equilibria and Diffusion*, *25*(4), 373–381.

Righter, K., Neff, K. E., and K.E. Neff. (2007). Temperature and oxygen fugacity constraints on CK and R chondrites and implications for water and oxidation in the early solar system. *Polar Science*, *1*(1), 25–44.

Righter, Kevin, and Drake, M. J. (1996). Core formation in Earth's moon, Mars, and Vesta. *Icarus*, *124*(2), 513–529.

Righter, Kevin, Sutton, S. R., Danielson, L., Pando, K., and Newville, M. (2016). Redox variations in the inner solar system with new constraints from vanadium XANES in spinels. *American Mineralogist*, *101*(9), 1928–1942.

Rose-Weston, L., Brenan, J. M., Fei, Y., Secco, R. A., and Frost, D. J. (2009). Effect of pressure, temperature, and oxygen fugacity on the metal-silicate partitioning of Te, Se, and S: Implications for earth differentiation. *Geochimica et Cosmochimica Acta*, *73*(15), 4598–4615.

Scheinberg, A., Elkins-Tanton, L. T., Schubert, G., and Bercovici, D. (2016). Core solidification and dynamo evolution in a mantle-stripped planetesimal. *Journal of Geophysical Research: Planets*, *121*(1), 2–20.

Scherstén, A., Elliott, T., Hawkesworth, C., Russell, S., and Masarik, J. (2006). Hf-W evidence for rapid differentiation of iron meteorite parent bodies. *Earth and Planetary Science Letters*, *241*(3–4), 530–542.

Schrader, D. L., McCoy, T. J., and Gardner-Vandy, K. (2017). Relict chondrules in primitive achondrites: Remnants from their precursor parent bodies. *Geochimica et Cosmochimica Acta*, *205*, 295–312.

Schulz, T., Upadhyay, D., Münker, C., and Mezger, K. (2012). Formation and exposure history of non-magmatic iron meteorites and winonaites: Clues from Sm and W isotopes. *Geochimica et Cosmochimica Acta*, *85*, 200–212.

Steenstra, E. S., Knibbe, J. S., Rai, N., and van Westrenen, W. (2016). Constraints on core formation in Vesta from metal-silicate partitioning of siderophile elements. *Geochimica et Cosmochimica Acta*, *177*, 48–61.

Stewart, A. J., and Schmidt, M. W. (2007). Sulfur and phosphorus in the Earth's core: The Fe-P-S system at 23 GPa. *Geophysical Research Letters*, *34*(13), 5–9.

Suer, T. A., Siebert, J., Remusat, L., Menguy, N., and Fiquet, G. (2017). A sulfur-poor terrestrial core inferred from metal–silicate partitioning experiments. *Earth and Planetary Science Letters*, *469*, 84–97.

Terasaki, H., Frost, D. J., Rubie, D. C., and Langenhorst, F. (2008). Percolative core formation in planetesimals. *Earth and Planetary Science Letters*, *273*(1–2), 132–137.

Ulff-Møller, F. (1998). Effects of liquid immiscibility on trace element fractionation in magmatic iron meteorites: A case study of group IIIAB. *Meteoritics and Planetary Science*, *33*(2), 207–220.

Wade, J., Wood, B. J., and Tuff, J. (2012). Metal-silicate partitioning of Mo and W at high pressures and temperatures: Evidence for late accretion of sulphur to the Earth. *Geochimica et Cosmochimica Acta*, *85*, 58–74.

Wadhwa, M. (2008). Redox Conditions on Small Bodies, the Moon and Mars. *Reviews in Mineralogy and Geochemistry*, *68*(1), 493–510.

Waldner, P., and Pelton, A. D. (2005). Thermodynamic Modeling of the Fe-S System. *Journal of Phase Equilibria and Diffusion*, *26*, 23–38.

Walker, D., Norby, L., and Jones, J. H. (1993). Superheating effects on metal-silicate partitioning of siderophile elements. *Science*, *262*(5141), 1858–1861.

Walker, R. J., McDonough, W. F., Honesto, J., Chabot, N. L., McCoy, T. J., Ash, R. D., and Bellucci, J. J. (2008). Modeling fractional crystallization of group IVB iron meteorites. *Geochimica et Cosmochimica Acta*, *72*(8), 2198–2216.

Wang, Z., and Becker, H. (2017). Chalcophile elements in Martian meteorites indicate low sulfur content in the Martian interior and a volatile element-depleted late veneer. *Earth and Planetary Science Letters*, *463*, 56–68.

Wasson, J. T., and Kallemeyn, G. W. (2002). The IAB iron-meteorite complex: A group, five subgroups, numerous grouplets, closely related, mainly formed by crystal segregation in rapidly cooling melts. *Geochimica et Cosmochimica Acta*, *66*(13), 2445–2473.

Wasson, J. T., and Richardson, J. W. (2001). Fractionation frends among IVA iron meteorites: Constrast with IIIAB trends. *Geochimica et Cosmochimica Acta*, *65*(6), 951–970.

Wasson, John T. (1999). Trapped melt in IIIAB irons; solid/liquid elemental partitioning during the fractionation of the IIIAB magma. *Geochimica et Cosmochimica Acta*, *63*(18), 2875–2889.

Wasson, John T., and Huber, H. (2006). Compositional trends among IID irons; their possible formation from the P-rich lower magma in a two-layer core. *Geochimica et Cosmochimica Acta*, *70*(24), 6153–6167.

Wasson, John T., Huber, H., and Malvin, D. J. (2007). Formation of IIAB iron meteorites. *Geochimica et Cosmochimica Acta*, *71*(3), 760–781.